


Critically enhanced spin-nematic squeezing and entanglement in dipolar spinor condensatesQing-Shou Tan ^{1,2} Yixiao Huang,³ Qiong-Tao Xie,² and Xiaoguang Wang⁴¹Key Laboratory of Hunan Province on Information Photonics and Freespace Optical Communications, Hunan Institute of Science and Technology, Yueyang 414000, China²College of Physics and Electronic Engineering, Hainan Normal University, Haikou 571158, China³School of Science, Zhejiang University of Science and Technology, Hangzhou, Zhejiang 310023, China⁴Department of Physics, Zhejiang Institute of Modern Physics, Zhejiang University, Hangzhou 310027, China

(Received 27 May 2020; accepted 17 September 2020; published 7 October 2020)

We study the quantum critical effect enhanced spin-nematic squeezing and quantum Fisher information (QFI) in the spin-1 dipolar atomic Bose-Einstein condensate. We show that the quantum phase transitions can improve the squeezing and QFI in the nearby regime of the critical point, and the Heisenberg-limited high-precision metrology can be obtained. The different properties of the ground squeezing and entanglement under even and odd number of atoms are further analyzed, by calculating the exact analytical expressions. We also demonstrate the squeezing and entanglement generated by the spin-mixing dynamics around the phase-transition point. It is shown that the steady squeezing and entanglement can be obtained, and the Bogoliubov approximation can well describe the dynamics of spin-nematic squeezed vacuum state.

DOI: [10.1103/PhysRevA.102.043307](https://doi.org/10.1103/PhysRevA.102.043307)**I. INTRODUCTION**

Spin squeezing has attracted much attention in precision metrology since it was first established by Kitagawa and Ueda [1]. In the past two decades, spin-squeezed states have been widely used in high-precision measurements to beat the standard quantum limit (SQL) [2–8] which is the best estimation limit of separable states with N particles and the scale is $1/\sqrt{N}$. In Ref. [1], two different mechanisms were proposed to generate spin-squeezed states: one-axis twisting (OAT) and two-axis twisting (TAT). The precision allowed by OAT and TAT states scales with $1/N^{2/3}$ and $1/N$, respectively. The best precision of TAT squeezed states is known as the Heisenberg scaling. In experiments, the TAT squeezed states are hard to achieve, whereas the OAT ones have been applied in Ramsey spectroscopy, atom interferometers, and high-precision atomic clocks.

The nonlinearity of Bose-Einstein condensates (BECs) caused by atomic collisions can create spin-squeezed states and is proved to be an ideal candidate for high-resolution quantum metrology [9,10]. In particular, the spinor atomic BECs have arisen much interest [11–18] due to their significant roles in studying the quantum metrology of many-body spin systems. Basically, these works can be sorted into two categories: spin-1/2 and integer-spin atomic systems. Compared with spin-1/2 atoms, whose states can be uniquely specified by different components of the total spin vector $\hat{S} = (\hat{S}_x, \hat{S}_y, \hat{S}_z)$, spin-1 atoms require additional spinor degrees of freedom to describe, associated with the quadrupole or nematic tensor operator \hat{Q}_{ij} ($i, j \in x, y, z$) [19–25]. These additional degrees of freedom concomitantly offer more degrees of freedom to squeezing and entanglement. Recently, the spin-nematic squeezing was observed in experiment by

the nonlinear collisional dynamics of spinor BEC, and the squeezing can be improved on the SQL by up to 8–10 dB [19].

In spinor atomic BECs, besides nonlinear collisional interactions, there is also long-range magnetic dipole-dipole interaction (MDDI) [26–35]. According to the recent experimental and theoretical observation in ^{23}Na , ^{87}Rb , and ^{52}Cr atoms, the MDDIs are, indeed, not negligible for these spinor condensates. Particularly, the achievements in spinor BECs provide a highly tunable and controllable system where the spin interactions, including the MDDI, can be accurately engineered [26,27,30,36]. The relative strength of the dipolar interaction and the spin exchange interaction describes a rich phase diagram [27,28,35]. These transitions between different phases are of interest with respect to spin squeezing and entanglement.

The present paper concerns generating highly spin-nematic squeezing and metrologically useful entanglement in different phases of spin-1 dipolar condensate including an ensemble of N atoms. Both the ground states and the dynamical behavior for them are considered. As the same as the usual spin squeezing, in spin-nematic squeezing, entanglement is also induced in an ensemble of atomic spins. Quantum Fisher information (QFI) [37,38], which plays a central role in quantum metrology, is able to detect useful multipartite entanglement. It is proved that QFI can perform even better than the spin-squeezing parameter in the detection of non-Gaussian states [39]. Thus, we can characterize the metrologically useful entanglement with QFI. In the SQL, the QFI $F \propto N$ is reached when uncorrelated atoms are used, whereas in the Heisenberg limit (HL), $F \propto N^2$ is possible by using entangled states.

Under our considered system, in the ground-state case, there are three sharp changes for both the squeezing and the QFI at the phase-transition points. More specifically, with

the change in MDDI, the QFI ranges from unentangled state scaled as N to a highly entangled state scaled, such as N^2 . It enables precision metrology to reach the Heisenberg scalar. The optimal squeezing, similar to TAT $\propto 1/N$, can occur nearby the regimes of vanished MDDI but at where the behavior is quite different for even and odd N . In the dynamics case, we focus on the steady squeezing nearby the critical point at which the spin transfer rates are very low. In this case, it is possible to obtain an analytical prediction for the spin-nematic squeezed vacuum state and QFI by adopting the Bogoliubov approximation. We also show that the analytical results are in well agreement with the numerical calculations. Our results shed new light on obtaining metrologically useful entanglement to improve the precision of quantum metrology using spinor BECs.

This paper is organized as follows. In Sec. II, we introduce the physical model of a spin-1 dipolar condensate and present the spin-nematic squeezing parameter and QFI. In Secs. III and IV, we study the critical effect enhanced spin-nematic squeezing and QFI in the cases of ground states and dynamics, respectively. Finally, a conclusion will be presented in Sec. V.

II. FORMULATION

A. Model

We consider a trapped gas of N bosonic atoms with hyperfine spin $f = 1$. Atoms interact via s -wave collisions and dipolar interaction. Assuming all spin components share a common spatial mode $\phi(r)$, under the single-mode approximation, the total spin-dependent Hamiltonian reads [27–29]

$$\hat{H} = (c'_2 - c'_d)\hat{S}^2 + 3c'_d\hat{S}_z^2 + 3c'_d\hat{a}_0^\dagger\hat{a}_0. \quad (1)$$

The total many-body angular momentum operator is $\hat{S} = \sum_{\alpha,\beta} \hat{a}_\alpha \mathbf{F}_{\alpha\beta} \hat{a}_\beta$ ($\alpha, \beta \in 0, \pm 1$) with \mathbf{F} being the spin-1 matrices and \hat{a}_α being the annihilation operator associated with the condensate mode, and the magnetization is defined as $S_z = \hat{a}_1^\dagger \hat{a}_1 - \hat{a}_{-1}^\dagger \hat{a}_{-1}$. The rescaled collisional and dipolar interaction strengths, respectively, are given by $c'_2 = (c_2/2) \int dr |\phi(r)|^4$ and $c'_d = (c_d/4) \int dr dr' |\phi(r)|^2 |\phi(r')|^2 (1 - 3 \cos^2 \theta_e) / |\vec{r} - \vec{r}'|^3$ with θ_e being the polar angle of $(\vec{r} - \vec{r}')$. Here, $c_2 = 4\pi \hbar^2 (a_2 - a_0) / (3M)$ with M being the mass of the atom, and $a_{0,2}$ being the s -wave scattering length for two spin-1 atoms in the symmetric channel of the total spin 0 and 2, respectively. The strength of the MDDI is given by $c_d = \mu_0 g_F^2 \mu_B^2 / 4\pi$ with μ_B as the Bohr magneton and g_F as the Landé g factor.

To proceed, it is convenient to rescale the Hamiltonian by using $|c'_2|$ as the energy unit, which yields the dimensionless Hamiltonian,

$$\hat{H}/|c'_2| = (\pm 1 - c)\hat{S}^2 + 3c\hat{S}_z^2 + 3c\hat{a}_0^\dagger\hat{a}_0. \quad (2)$$

The sign of “+” (“−”) corresponding to $c'_2 > 0$ ($c'_2 < 0$), which is determined by the type of atoms: for $c'_2 < 0$ (as for ^{87}Rb) the interaction term favors the ferromagnetic phase; whereas for $c'_2 > 0$ (as for ^{23}Na), the antiferromagnetic phase minimizes the interaction energy. Here, $c \equiv c'_d/|c'_2|$ is the relative strength of the dipolar interaction with respect to the spin exchange interaction and is treated as a control parameter.

Fortunately, the sign and magnitude of the dipolar interaction strength c'_d can be tuned via modifying the trapping geometry [27] or a quick rotating orienting field [30], and the contact interaction strength c'_2 is also tunable via Feshbach resonance. Without loss generally, throughout this paper, we focus on the case of antiferromagnetic Bose-Einstein condensate such that $c'_2 > 0$.

Due to the dipolar interaction, more new quantum phases can be found by tuning the values of c [27]. The c -dependence ground state of Hamiltonian (2) can be found by minimizing $\langle \hat{H} \rangle$ in the $|S, m\rangle$ basis, which is defined by

$$\hat{S}^2 |S, m\rangle = s(s+1) |S, m\rangle, \quad \hat{S}_z |S, m\rangle = m |S, m\rangle, \quad (3)$$

where $m = 0, \pm 1, \dots, \pm S$. For a given total number of atoms N , the allowable values of S are $S = 0, 2, 4, \dots, N$ for even N , and $S = 1, 3, 5, \dots, N$ for odd N .

B. Spin-nematic squeezing parameter and quantum Fisher information

In the case of spin-1 atomic Bose-Einstein condensates, the multipolar moments can be specified in terms of both the spin vector \hat{S}_i and nematic tensor \hat{Q}_{ij} ($i, j \in x, y, z$) which constitute SU(3) Lie algebra. Based on the definition of the operator \hat{Q}_{ij} [19–22],

$$\begin{aligned} \hat{Q}_{yz} &= \frac{i}{\sqrt{2}} (-\hat{a}_1^\dagger \hat{a}_0 + \hat{a}_0^\dagger \hat{a}_{-1} + \hat{a}_0^\dagger \hat{a}_1 - \hat{a}_{-1}^\dagger \hat{a}_0), \\ \hat{Q}_{xz} &= \frac{1}{\sqrt{2}} (\hat{a}_1^\dagger \hat{a}_0 - \hat{a}_0^\dagger \hat{a}_{-1} + \hat{a}_0^\dagger \hat{a}_1 - \hat{a}_{-1}^\dagger \hat{a}_0), \\ \hat{Q}_{xx} &= \frac{2}{3} \hat{a}_0^\dagger \hat{a}_0 - \frac{1}{3} \hat{a}_1^\dagger \hat{a}_1 - \frac{1}{3} \hat{a}_{-1}^\dagger \hat{a}_{-1} + \hat{a}_1^\dagger \hat{a}_{-1} + \hat{a}_{-1}^\dagger \hat{a}_1, \\ \hat{Q}_{yy} &= -\frac{1}{3} \hat{a}_1^\dagger \hat{a}_1 + \frac{2}{3} \hat{a}_0^\dagger \hat{a}_0 - \frac{1}{3} \hat{a}_{-1}^\dagger \hat{a}_{-1} - \hat{a}_1^\dagger \hat{a}_{-1} - \hat{a}_{-1}^\dagger \hat{a}_1, \\ \hat{Q}_{zz} &= \frac{2}{3} \hat{a}_1^\dagger \hat{a}_1 - \frac{4}{3} \hat{a}_0^\dagger \hat{a}_0 + \frac{2}{3} \hat{a}_{-1}^\dagger \hat{a}_{-1}, \end{aligned}$$

there are two different spin-nematic squeezing parameters in the SU(2) subspaces, $\{\hat{S}_x, \hat{Q}_{yz}, \hat{Q}_{zz} - \hat{Q}_{yy}\}$ and $\{\hat{S}_y, \hat{Q}_{xz}, \hat{Q}_{xx} - \hat{Q}_{zz}\}$, which are defined by [19,22]

$$\xi_{x(y)}^2 = \frac{2[\langle \Delta(S_{x(y)} \cos \varphi + Q_{yz(xz)} \sin \varphi) \rangle^2]_{\min}}{|\langle \hat{Q}_{zz} - \hat{Q}_{yy(xx)} \rangle|}, \quad (4)$$

where the minimization is over all the quadrature angle φ . A state is spin nematic squeezed if $\xi_{x(y)}^2 < 1$.

Below, we focus on the squeezing in the $\{S_x, Q_{yz}, Q_+\}$ subspace with $\hat{Q}_+ = \hat{Q}_{zz} - \hat{Q}_{yy}$. The spin-nematic squeezing parameter may be reduced as

$$\xi_x^2 = \frac{A - \sqrt{B^2 + C^2}}{|\langle \hat{Q}_+ \rangle|}, \quad (5)$$

by finding the optimal squeezing angle,

$$\varphi_{\text{opt}} = \begin{cases} \frac{1}{2} \arccos\left(\frac{-B}{\sqrt{B^2 + C^2}}\right), & B \leq 0, \\ \pi - \frac{1}{2} \arccos\left(\frac{-B}{\sqrt{B^2 + C^2}}\right), & B > 0, \end{cases}$$

where we define

$$\begin{aligned} A &= \langle S_x^2 + Q_{yz}^2 \rangle, & B &= \langle S_x^2 - Q_{yz}^2 \rangle, \\ C &= \langle S_x Q_{yz} + Q_{yz} S_x \rangle. \end{aligned} \quad (6)$$

A wide variety of spin-squeezing techniques have been used to show sub-SQL of metrological sensitivity. To better understand the behavior of enhanced metrological sensitivity, we can evaluate the QFI in the $\hat{\Lambda} = \{\hat{S}_x, \hat{Q}_{yz}, \hat{Q}_+\}$ subspace.

According to Refs. [4,25,40–43], the QFI F with respect to measured phase θ , acquired by an SU(2) rotation on the input state $\hat{\rho}_{\text{in}}$, can be explicitly derived as

$$F[\hat{\rho}(\theta), \hat{\Lambda}_{\vec{n}}] = \vec{n} C \vec{n}^T, \quad (7)$$

where

$$\hat{\rho}(\theta) = \exp(-i\theta \hat{\Lambda}_{\vec{n}}) \hat{\rho}_{\text{in}} \exp(i\theta \hat{\Lambda}_{\vec{n}}), \quad (8)$$

with $\hat{\Lambda}_{\vec{n}} = \hat{\Lambda} \cdot \vec{n}$ being the generator of rotation and \vec{n} being the unit length vector. Here, the matrix element for the symmetric matrix C is

$$C_{kl} = \sum_{i \neq j} \frac{(p_i - p_j)^2}{p_i + p_j} [\langle i | \Lambda_k | j \rangle \langle j | \Lambda_l | i \rangle + \langle i | \Lambda_l | j \rangle \langle j | \Lambda_k | i \rangle],$$

where $p_i(i)$ are the eigenvalues (eigenvectors) of $\hat{\rho}(\theta)$. From Eq. (7), one finds that to get the highest possible estimation precision θ , a proper direction \vec{n} should be chosen for a given state, which maximizes the value of the QFI. With the help of the symmetric matrix, then, the maximal QFI in the $\{\hat{S}_x, \hat{Q}_{yz}, \hat{Q}_+\}$ subspace can be obtained as

$$\begin{aligned} F_{\text{max}} &= 4 \max \{ (\Delta \Lambda_{\perp})_{\text{max}}^2, (\Delta Q_+/2)^2 \} \\ &= \max \{ 2(A + \sqrt{B^2 + C^2}), (\Delta Q_+)^2 \}, \end{aligned} \quad (9)$$

$$\sqrt{B^2 + C^2} = 4 \sum_{m,k} |g_{m,k} g_{m,k+1}| \sqrt{(N-2k+m-1)(N-2k+m)(k+1)(k+1-m)}. \quad (12)$$

We can also find the expectation value of Q_+ ,

$$\langle Q_+ \rangle = \sum_{m,k} g_{m,k}^2 (6k - 2N - 3m), \quad (13)$$

as well as the corresponding fluctuation,

$$\begin{aligned} (\Delta Q_+)^2 &= 9 \left[\sum_{m,k} g_{m,k}^2 (2k - m)^2 - \left(\sum_{m,k} g_{m,k}^2 (2k - m) \right)^2 \right] \\ &+ \sum_{m,k} g_{m,k}^2 [2k(k+1) - m(2k+1)]. \end{aligned} \quad (14)$$

Substituting the above equations into Eqs. (5) and (9), we can obtain the spin-nematic squeezing and QFI in the case of ground states.

Figures 1 and 2 illustrate the c dependence of the spin-nematic squeezing ($10 \log_{10} \xi_x^2$) and QFI for $N = 100$ (even number) and $N = 101$ (odd number), respectively. From Figs. 1 and 2, we can see there are three sharp changes for

where $\langle Q_+ \rangle$ is normalized by dividing 2 since $|\langle Q_+ \rangle|_{\text{max}} = 2N$. In Eq. (9), the maximal possible value of the QFI is $F = 4N^2$, which can be obtained only by the fully particle entangled states. On the other hand, separable states can give at most $F = 4N$, such as $|0, N, 0\rangle$ state. The factor 4 in the scaling of characteristic limits of the QFI is due to SU(3) Lie algebra [25]. In terms of the definition in Eq. (9), a state is entangled in the $\{\hat{S}_x, \hat{Q}_{yz}, \hat{Q}_+\}$ subspace if QFI $F > 4N$.

In what follows, we will study the spin-nematic squeezing and QFI in the cases of ground states and spin-mixing dynamics, respectively, when $c'_2 > 0$.

III. SPIN-NEMATIC SQUEEZING AND QUANTUM FISHER INFORMATION IN GROUND STATES

Now, we will consider the spin-nematic squeezing and QFI in the case of ground states. Numerically, it is convenient to expand the ground state as

$$|G\rangle = \sum_{m,k} g_{m,k} |m, k\rangle, \quad (10)$$

in the Fock basis $|m, k\rangle \equiv |N_1, N_0, N_{-1}\rangle$ with the notations $N_1 = k$, $N_0 = N - 2k + m$, and $N_{-1} = k - m$. Here, $m = -N, -N + 1, \dots, N$ for a given m , the allowable values of k satisfy the relation $\max(0, m) \leq k \leq \text{Int}[\frac{N+m}{2}]$, where $\text{Int}[x]$ is a function for getting the integer part of x . Since Hamiltonian (2) commutes with \hat{S}_z , the ground state must lie in a certain m subspace, then, the matrix elements of Hamiltonian (2) become $H_{m,k,m,k'} = \langle m, k | H | m, k' \rangle$. The amplitudes $g_{m,k}$ can be obtained just by numerically diagonalizing the Hamiltonian. Hence, the expectation values given in Eq. (6) read

$$A = \sum_{m,k} g_{m,k}^2 [(2N - 4k + 2m - 1)(2k - m) + 2N], \quad (11)$$

and

both the squeezing and the QFI when $c = -0.5$, $c = 0$, and $c = 1$. The squeezing can be found in the region $-0.5 < c < 1$. When $c < -0.5$, there is neither squeezing ($\xi_x^2 = 1$) nor entanglement ($F^{\text{max}} = 2N$) since the ground state is a Fock state with all the population in either the $m_f = 1$ or -1 state for both the even and the odd N . When $c \geq 1$, there is no squeezing ($\xi_x^2 \geq 1$) but highly entangled states. For instance, when $c = 1$, $|G\rangle = |N/2, 0, N/2\rangle$ (assuming N to be even) is the twin-Fock state [15,44–46], which is a deeply entangled state in the picture of particles. Recently, Luo *et al.* demonstrated near-deterministic generation of this state of 11 000 atoms in ^{87}Rb BEC [15]. Whereas for $c > 1$, $|G\rangle \approx |S = N, m = 0\rangle$ is the so-called Dicke state [16,27,47] which is a massively entangled state of all the atoms ($F^{\text{max}} \approx 2N^2$). Zhang and Duan [16] have proposed a robust method to generate this state in a spinor BEC. From Fig. 1, we can clearly find that the optimal squeezing occurs around $c = 0$, but the behavior is different for even and odd N in this regime. Actually, for $c = 0$, the spin-nematic squeezing is not well defined for even

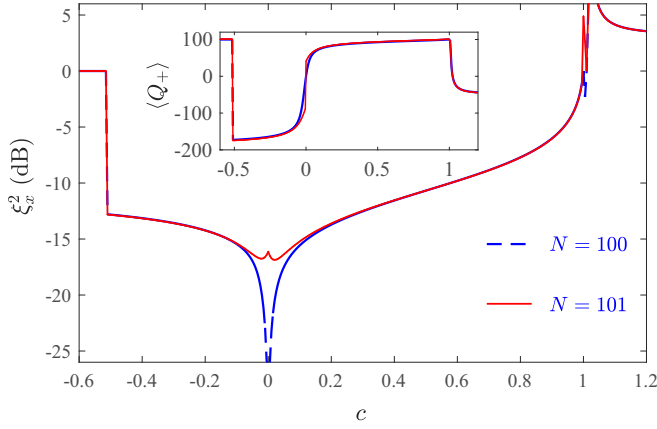


FIG. 1. The c dependence of the spin-nematic squeezing ξ_x^2 for $N = 100$ and $N = 101$. The inset shows its $\langle Q_+ \rangle$ with respect to c .

N , therefore, we should discuss the results for even and odd N separately when $c = 0$.

For $c = 0$ and even N , the ground-state $|G\rangle$ is the spin-singlet state [11],

$$|S = 0, m = 0\rangle = \sum_{k=0}^{N/2} \tilde{g}_k |k, N - 2k, k\rangle, \quad (15)$$

with $\tilde{g}_k \equiv g_{0,k}$ where the amplitudes obey the recursion relation,

$$\tilde{g}_0 = \frac{1}{\sqrt{N+1}}, \quad \tilde{g}_k = -\sqrt{\frac{N-2k+2}{N-2k+1}} \tilde{g}_{k-1}. \quad (16)$$

After computing the recursion relation, we get

$$\tilde{g}_k = \frac{(-1)^k}{\sqrt{N+1}} \prod_{x=0}^{k-1} \sqrt{\frac{N-2x}{N-2x-1}}. \quad (17)$$

The spin-singlet state is a quantum superposition of a chain of Fock states in which the number of atoms in state $m_f = \pm 1$ is equal. To get some insight, we first calculate the expectation

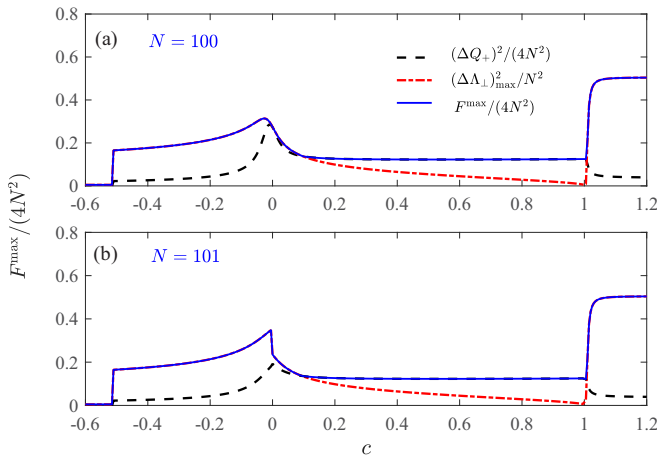


FIG. 2. The c dependence of the maximal QFI divided by $4N^2$ for (a) $N = 100$ and (b) $N = 101$.

values given in Eqs. (6) for this state, which yields

$$A = \sqrt{B^2 + C^2} = \frac{4N(N+3)}{15}, \quad (18)$$

and the expectation value of Q_+ is $\langle Q_+ \rangle = 0$. Thus, the spin-nematic squeezing parameter of the spin-singlet state is the 0/0 type. It is undefined at this point for even N , although the squeezing is strongest when $c \rightarrow 0$ (as shown in Fig. 1). However, it has QFI, and the optimal value is

$$\begin{aligned} F^{\max} &= (\Delta Q_+)^2 = 4(\Delta \Lambda_{\perp})_{\max}^2 \\ &= \frac{16N(N+3)}{15}, \end{aligned} \quad (19)$$

which is the Heisenberg scalar. It indicates that the spin-singlet state features genuine multipartite entanglement of the entire ensemble and will be useful for quantum metrology. This conclusion is consistent with the earlier paper reported by Tóth [48].

For $c = 0$ and odd N , the ground state is $|G\rangle = |S = 1, m = 0\rangle$ which is given by

$$|S = 1, m = 0\rangle = c_0 \sum_{k=0}^n c_k |k, N - 2k, k\rangle. \quad (20)$$

After computing the recursion relation, the amplitudes read

$$c_k = (-1)^k \sqrt{\frac{3(2n-2k+1)}{(k+1)}} \prod_{x=0}^{k-1} \sqrt{\frac{(x+2)(2n-2x)}{(x+1)(2n-2x-1)}}, \quad (21)$$

and the normalization constant c_0 is given by

$$c_0 = \left(\sum_{k=0}^n c_k^2 \right)^{-1/2} = \frac{1}{\sqrt{4n^2 + 8n + 3}}, \quad (22)$$

with $n = (N-1)/2$.

By substituting the ground-state $|S = 1, m = 0\rangle$ into Eqs. (6), we find

$$\langle Q_+ \rangle = -\frac{4N+6}{5}, \quad (23a)$$

$$(\Delta Q_+)^2 = \frac{128(N-1)(N+4)}{175}, \quad (23b)$$

$$A = \frac{12N^2 + 36N + 12}{35}, \quad (23c)$$

$$\sqrt{B^2 + C^2} = \frac{12N^2 + 36N - 48}{35}. \quad (23d)$$

Then, the value of spin-nematic squeezing is

$$\xi_x^2 = \frac{5}{2N+3}. \quad (24)$$

This squeezing value is quite similar to the TAT case which $\propto 1/N$ for $N \gg 1$ [1]. According to Eq. (9), the maximal QFI of ground-state $|S = 1, m = 0\rangle$ is

$$F^{\max} = 4(\Delta \Lambda_{\perp})_{\max}^2 = \frac{48N(N+3)}{35} - \frac{72}{35}, \quad (25)$$

TABLE I. The ground-state $|G\rangle$, the spin-nematic squeezing ξ_x^2 , the maxima QFI F^{\max} around the critical points $c < -0.5$, $c = 0$, $c \geq 1$ for even N .

c	< -0.5	0	1	> 1
$ G\rangle$	$ N, \pm N\rangle$	$ 0, 0\rangle$	$ \frac{N}{2}, 0, \frac{N}{2}\rangle$	$\approx N, 0\rangle$
ξ_x^2	1	Undefined	1	> 1
F^{\max}	$2N$	$\frac{16N(N+3)}{15}$	$\frac{N^2}{2} + N$	$\approx 2N^2$

which also is the Heisenberg scalar. To better show these results, Tables I and II lists the ground states $|G\rangle$, the spin-nematic squeezing parameter ξ_x^2 , and the maximal QFI F^{\max} around the critical points for even (odd) N .

IV. SPIN-NEMATIC SQUEEZING AND QUANTUM FISHER INFORMATION DYNAMICS

We, now, turn to study the spin-nematic squeezing and QFI generated by the spin-mixing dynamics of the dipolar spinor condensate with even N .

A. Numerical results

The spin-mixing dynamics generated squeezing and QFI can be studied by numerically evolving an initial state under the total spin-dependent Hamiltonian. Here, we consider two different initial states of the system, namely, $|0, N, 0\rangle$ and $|N/2, 0, N/2\rangle$, and, then, let the states become free dynamic evolution. Hamiltonian (2) conserves both the total particle number N and magnetization S_z , in general, the evolution states have the form

$$|\Psi(t)\rangle = \sum_{k=0}^{N/2} g_k(t)|k\rangle, \quad (26)$$

where $|k\rangle \equiv |k, N - 2k, k\rangle$ represents the Fock state.

Here, the spin-nematic squeezing parameter can be reduced to

$$\xi_x^2 = \frac{A' - 2|B'|}{|3\langle a_1^\dagger a_1 \rangle - N|}, \quad (27)$$

with $\langle a_1^\dagger a_1 \rangle = \sum_{k=0}^{N/2} |g_k|^2 k$ and

$$A' = \sum_{k=0}^{N/2} |g_k|^2 [(k+1)(N-2k) + (N-2k+1)k], \quad (28a)$$

TABLE II. The ground-state $|G\rangle$, the spin-nematic squeezing ξ_x^2 , the maxima QFI F^{\max} around the critical points $c < -0.5$, $c = 0$, $c \geq 1$ for odd N .

c	< -0.5	0	1	> 1
$ G\rangle$	$ S, \pm N\rangle$	$ 1, 0\rangle$	$ \frac{N+1}{2}, 0, \frac{N-1}{2}\rangle$	$\approx N, 0\rangle$
ξ_x^2	1	$\frac{5}{2N+3}$	1	> 1
F^{\max}	$2N$	$\frac{48N(N+3)-72}{35}$	$\frac{N^2-1}{2} + N$	$\approx 2N^2$

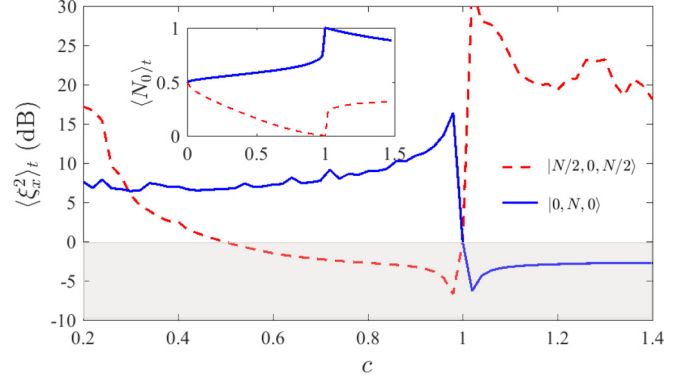


FIG. 3. The c dependence of the time average of $\langle \xi_x^2 \rangle_t$ for two different initial states $|0, N, 0\rangle$ and $|N/2, 0, N/2\rangle$ with $N = 2000$. The shaded area indicates the region of squeezed states. The inset shows the time average of the population for the $m_f = 0$ component.

$$B' = \sum_{k=1}^{N/2} g_k^* g_{k-1} k \sqrt{(N-2k+2)(N-2k+1)}. \quad (28b)$$

We can also find the maximal QFI as

$$F^{\max} = \max\{4(A' + 2|B'|), (\Delta Q_+)^2\}, \quad (29)$$

where

$$(\Delta Q_+)^2 = 2 \sum_k^{N/2} |g_k|^2 k(k+19) - 36 \left(\sum_k^{N/2} |g_k|^2 k \right)^2. \quad (30)$$

The spin-mixing dynamics will quickly drive the system into a quasisteady state [11, 12, 27], that is, the average number of atoms in the spin components will remain unchanged for a long time. The c dependence of the quasi-steady-state squeezing as well as population of the $m_f = 0$ component for two different initial states $|0, N, 0\rangle$ and $|N/2, 0, N/2\rangle$ are plotted in Fig. 3. As shown in Fig. 3, the quasi-steady-state behavior display a sudden change when $c \rightarrow 1$. For initial-state $|0, N, 0\rangle$, we can get steady squeezing (≈ -5 dB) in the regime of $c > 1$, whereas the case for initial-state $|N/2, 0, N/2\rangle$ will be the opposite. The detailed dynamical behaviors of the squeezing for these states around the critical point $c = 1$ are shown in Fig. 4. As is shown, the spin-nematic squeezing can be improved on the SQL by up to 20 dB around the critical point before reaching the steady squeezing.

We note that the preparation of highly entangled ideal twin-Fock state $|N/2, 0, N/2\rangle$ may pose an experimental challenge. Below, we focus on the case of initial states $|0, N, 0\rangle$ to understand the steady squeezing behavior shown in Figs. 3 and 4. In terms of the spin-nematic squeezing parameter given in Eq. (27), we can find that the squeezing depends on the atomic population. When $c \rightarrow 1$, there is essentially no population transfer from the mode $m_f = 0$ to the other two modes $m_f = \pm 1$, and, hence, $\langle N_0 \rangle / N \rightarrow 1$ which corresponds to squeezed vacuum for the $m_f = \pm 1$ modes [19–22]. Once c deviated from 1, as evolution time is increased, the ratio N_0/N will decrease until reach the quasisteady state due to the spin-mixing dynamics. In Fig. 5, we show the dynamical behavior of N_0/N as well as the corresponding squeezing. As is shown, when $c < 1$, the average number of atoms in the

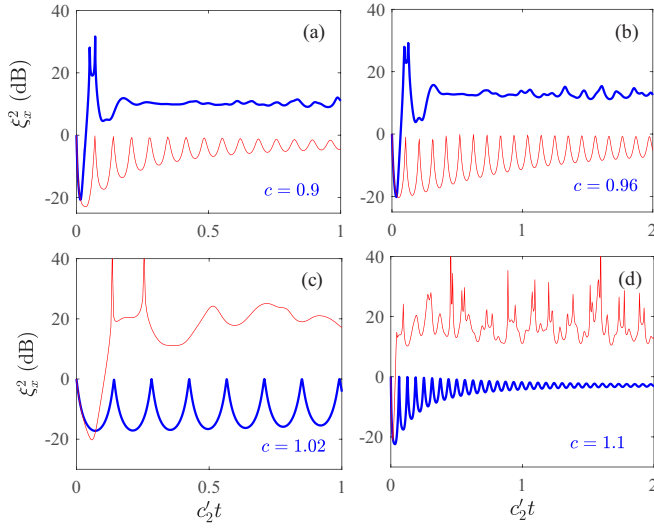


FIG. 4. Time dependence of the spin-nematic squeezing parameter ξ_x^2 for different initial states, $|0, N, 0\rangle$ (blue thick line) and $|N/2, 0, N/2\rangle$ (red thin line). Here, $N = 2000$.

$m_f = 0$ mode descend rapidly, and the spin-nematic squeezed vacuum only keeps for a very short time. Whereas $c > 1$, due to the small spin-mixing parameter $1 - c$ in Hamiltonian (2), the ratio N_0/N will fall slowly before reaching the quasisteady, like-damped oscillation. Corresponding to the evolution of N_0/N , there is a damped oscillations of the squeezing, and the quasisteady squeezing can be obtained. However, we should point out that the steady squeezing is not a spin-nematic squeezed vacuum, and it is a difficult task to write out the explicit form of them.

Next, we analytically analyze the dynamical behavior of the squeezed vacuum with the Bogoliubov approximation around $c \rightarrow 1$.

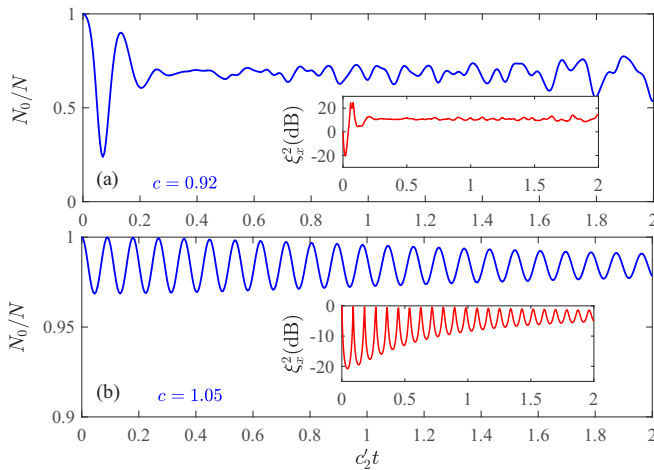


FIG. 5. Time dependence of average number of atoms in the $m_f = 0$ mode normalized by the total number of atoms N with different c . The insets show the correspondent spin-nematic squeezing parameter. The initial state of the system is $|0, N, 0\rangle$ with $N = 2000$.

B. Bogoliubov approximation

We, now, use the Bogoliubov approximation to replace the annihilation and creation operators for the condensate with number N , that is, $a_0 \approx a_0^\dagger \approx \sqrt{N}$. Up to phase factor that we may neglect since we are later concerned only with expectation values where the phase would cancel out. Therefore, we can introduce the operators,

$$K_x = \frac{1}{2}(a_1^\dagger a_{-1}^\dagger + a_1 a_{-1}), \quad K_y = -\frac{i}{2}(a_1^\dagger a_{-1}^\dagger - a_1 a_{-1}), \quad (31)$$

$$K_z = \frac{1}{2}(a_1^\dagger a_1 + a_{-1}^\dagger a_{-1}),$$

which belong to the $SU(1,1)$ group and satisfy $[K_x, K_y] = -iK_z$, $[K_y, K_z] = iK_x$ and $[K_z, K_x] = iK_y$.

Using the definitions in Eq. (31), the effective Hamiltonian of Eq. (2) is given by

$$H_{\text{eff}} \equiv \alpha K_z + \beta K_x, \quad (32)$$

with c -dependence parameters,

$$\alpha = 2[(1-c)(2N-1) - 3c], \quad \beta = 4(1-c)N. \quad (33)$$

In terms of the $SU(1,1)$ operators, Eq. (6) may be expressed as

$$A = 4N\langle K_z \rangle, \quad \sqrt{B^2 + C^2} = 4N|\langle K_+ \rangle|, \quad (34)$$

where $K_+ = K_-^\dagger = K_x + iK_y = a_1^\dagger a_{-1}^\dagger$. Therefore, the spin-nematic squeezing parameter and QFI can be reduced to

$$\xi_x^2 = 2\langle K_z \rangle - 2|\langle K_+ \rangle|, \quad (35)$$

$$F^{\text{max}} = 8N(\langle K_z \rangle + |\langle K_+ \rangle|), \quad (36)$$

since $\Delta Q_+ \rightarrow 0$.

To get the explicit form of both the squeezing and the QFI, we only need to calculate the expectation values $\langle K_z \rangle$ and $\langle K_+ \rangle$. With the help of the time-evolution operator $U(t) = \exp[-iH_{\text{eff}}t]$, we have

$$\begin{aligned} \langle K_z \rangle &= \langle 0, N, 0 | U^\dagger(t) K_z U(t) | 0, N, 0 \rangle \\ &= \frac{\Gamma_1(1 + \Gamma^2)}{2(1 - \Gamma^2)^2}, \end{aligned} \quad (37)$$

$$\begin{aligned} |\langle K_+ \rangle| &= |\langle 0, N, 0 | U^\dagger(t) K_+ U(t) | 0, N, 0 \rangle| \\ &= \frac{\Gamma_1 \Gamma}{(1 - \Gamma^2)^2}, \end{aligned} \quad (38)$$

where

$$\begin{aligned} \Gamma &= \frac{|\beta \sin(\theta t)|}{\sqrt{\alpha^2 - \beta^2 \cos^2(\theta t)}}, \quad \Gamma_1 = \frac{\alpha^2 - \beta^2}{\alpha^2 - \beta^2 \cos^2(\theta t)}, \\ \theta &= \frac{1}{2}\sqrt{\alpha^2 - \beta^2}. \end{aligned} \quad (39)$$

If $c > 1$, we have $\alpha^2 > \beta^2$, a direct calculation yields

$$\xi_x^2 = \frac{\Gamma_1}{(1 + \Gamma^2)}, \quad F^{\text{max}} = \frac{4N\Gamma_1}{(1 - \Gamma^2)^2}, \quad (40)$$

and the optical values are given by

$$(\xi_x^2)_{\text{min}} = \frac{|\alpha| - |\beta|}{|\alpha| + |\beta|} = \frac{2c + 1}{4N(c - 1) + 2c + 1}, \quad (41)$$

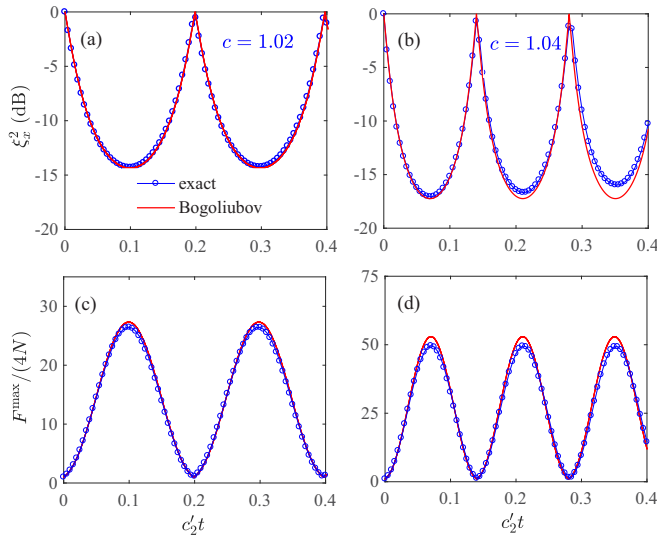


FIG. 6. Comparison of dynamical behaviors of ξ_x^2 (a) and (b) and $F^{\max}/(4N)$ (c) and (d) for the exact numerical solution and Bogoliubov approximate solution with different c 's. Here, $N = 1000$.

$$F^{\max}(t_{\text{opt}}) = \frac{4N(|\alpha| + |\beta|)}{|\alpha| - |\beta|} = \frac{4N}{(\xi_x^2)_{\min}}, \quad (42)$$

when $t_{\text{opt}} = \pi/\sqrt{\alpha^2 - \beta^2}$. The above results are valid when $c \rightarrow 1_+$, which corresponds to the spin-nematic squeezed vacuum.

Figure 6 shows the comparison of squeezing and QFI between the exact solutions and the Bogoliubov approximation for different c 's. As is shown, with the increasing of c , the squeezing and QFI are enhanced, and the Bogoliubov approximation solutions are in agreement with the exact ones when $c \rightarrow 1_+$. However, for a long time, the squeezing is not a squeezed vacuum as shown in Figs. 4 and 5, and, hence, the Bogoliubov approximation will be invalid.

V. CONCLUSION

To summarize, we have studied the spin-nematic squeezing and QFI under the ground state and spin-mixing dynamics of an antiferromagnetic spin-1 Bose-Einstein condensate, respectively. We have shown that the quantum phases which depend on the relative strengths of the spin exchange and dipolar interactions can generate highly entangled ground states in several limits, and enable precision metrology to reach the HL. We have also studied the quantum critical effect enhanced spin-nematic squeezing and entanglement in the dynamics case. It indicated that the spin-nematic squeezing can be enhanced to ≈ -20 dB before arriving the steady values ≈ -5 dB. We also demonstrated that the Bogoliubov approximation can well describe the dynamics of spin-nematic squeezed vacuum state.

Finally, it should be pointed out that our paper, here, has neglected any external magnetic field. The presence of external fields will affect the orientation of the spin and, hence, change the phase diagram. The effect of the magnetic field on spin-1 condensates without MDDI is currently under study [15,16,21]. The quantum phase transition due to the quadratic Zeeman shift may also demonstrate some similar squeezing behavior as our case. Therefore, the quantum critical effect enhanced spin-nematic squeezing and entanglement should also be expected in the case of the spinor BEC in an external magnetic.

ACKNOWLEDGMENTS

Q.-S.T. acknowledges support from the NSFC under Grants No. 11805047 and No. 11665010, and Hainan Science and Technology Plan Project (Grant No. ZDKJ2019005). Y.H. acknowledges support from the NSFC under Grant No. 11605157. Q.-T.X. acknowledges support from the NSFC under Grant No. 11965011. X.W. was supported by the National Natural Science Foundation of China (Grants No. 11875231 and No. 11935012), the National Key Research and Development Program of China (Grants No. 2017YFA0304202 and No. 2017YFA0205700), and the Fundamental Research Funds for the Central Universities (Grant No. 2018FZA3005).

-
- [1] M. Kitagawa and M. Ueda, Squeezed spin states, *Phys. Rev. A* **47**, 5138 (1993).
- [2] D. J. Wineland, J. J. Bollinger, W. M. Itano, F. L. Moore and D. J. Heinzen, Spin squeezing and reduced quantum noise in spectroscopy, *Phys. Rev. A* **46**, 6797(R) (1992).
- [3] D. J. Wineland, J. J. Bollinger, W. M. Itano and D. J. Heinzen, Squeezed atomic states and projection noise in spectroscopy, *Phys. Rev. A* **50**, 67 (1994).
- [4] J. Ma, X. Wang, C. P. Sun, and F. Nori, Quantum spin squeezing, *Phys. Rep.* **509**, 89 (2011).
- [5] L. Pezzé, A. Smerzi, M. K. Oberthaler, R. Schmied, and P. Treutlein, Quantum metrology with nonclassical states of atomic ensembles, *Rev. Mod. Phys.* **90**, 035005 (2018).
- [6] A. D. Cronin, J. Schmiedmayer and D. E. Pritchard, Optics and interferometry with atoms and molecules, *Rev. Mod. Phys.* **81**, 1051 (2009).
- [7] J. D. Sau, S. R. Leslie, M. L. Cohen, and D. M. Stamper-Kurn, Spin squeezing of high-spin, spatially extended quantum fields, *New J. Phys.* **12**, 085011 (2010).
- [8] G. Vitagliano, P. Hyllus, I. L. Egusquiza, and G. Tóth, Spin Squeezing Inequalities for Arbitrary Spin, *Phys. Rev. Lett.* **107**, 240502 (2011).
- [9] C. Gross, T. Zibold, E. Nicklas, J. Esteve, and M. K. Oberthaler, Nonlinear atom interferometer surpasses classical precision limit, *Nature (London)* **464**, 1165 (2010).
- [10] M. F. Riedel, P. Bohi, Y. Li, T. W. Hansch, A. Sinatra, and P. Treutlein, Atom-chip-based generation of entanglement for quantum metrology, *Nature (London)* **464**, 1170 (2010).
- [11] C. K. Law, H. Pu, and N. P. Bigelow, Quantum Spins Mixing in Spinor Bose-Einstein Condensates, *Phys. Rev. Lett.* **81**, 5257 (1998).

- [12] M.-S. Chang, Q. Qin, W. Zhang, and M. S. Chapman, Coherent spinor dynamics in a spin-1 Bose condensate, *Nat. Phys.* **1**, 111 (2005).
- [13] Y. Kawaguchi and M. Ueda, Spinor Bose-Einstein condensates, *Phys. Rep.* **520**, 253 (2012).
- [14] D. M. Stamper-Kurn and M. Ueda, Spinor Bose gases: Symmetries, magnetism, and quantum dynamics, *Rev. Mod. Phys.* **85**, 1191 (2013).
- [15] X. Y. Luo, Y. Q. Zou, L. N. Wu, Q. Liu, M. F. Han, M. K. Tey, and L. You, Deterministic entanglement generation from driving through quantum phase transitions, *Science* **355**, 620 (2017).
- [16] Z. Zhang and L.-M. Duan, Generation of Massive Entanglement Through an Adiabatic Quantum Phase Transition in a Spinor Condensate, *Phys. Rev. Lett.* **111**, 180401 (2013).
- [17] Ö. E. Müstecaplıoğlu, M. Zhang, and L. You, Spin squeezing and entanglement in spinor condensates, *Phys. Rev. A* **66**, 033611 (2002).
- [18] D. Kajtoch and E. Witkowska, Spin squeezing in dipolar spinor condensates, *Phys. Rev. A* **93**, 023627 (2016).
- [19] C. D. Hamley, C. S. Gerving, T. M. Hoang, E. M. Bookjans, and M. S. Chapman, Spin-nematic squeezed vacuum in a quantum gas, *Nat. Phys.* **8**, 305 (2012).
- [20] C. S. Gerving, T. M. Hoang, B. J. Land, M. Anquez, C. D. Hamley, and M. S. Chapman, Non-equilibrium dynamics of an unstable quantum pendulum explored in a spin-1 Bose-Einstein condensate, *Nat. Commun.* **3**, 1169 (2012).
- [21] T. M. Hoang, C. S. Gerving, B. J. Land, M. Anquez, C. D. Hamley, and M. S. Chapman, Dynamic Stabilization of a Quantum Many-Body Spin System, *Phys. Rev. Lett.* **111**, 090403 (2013).
- [22] Y. Huang, H. N. Xiong, Z. Sun, and X. Wang, Generation and storage of spin-nematic squeezing in a spinor Bose-Einstein condensate, *Phys. Rev. A* **92**, 023622 (2015).
- [23] S. J. Masson, M. D. Barrett, and S. Parkins, Cavity QED Engineering of Spin Dynamics and Squeezing in a Spinor Gas, *Phys. Rev. Lett.* **119**, 213601 (2017).
- [24] S. J. Masson and S. Parkins, Rapid Production of Many-Body Entanglement in Spin-1 Atoms Via Cavity Output Photon Counting, *Phys. Rev. Lett.* **122**, 103601 (2019).
- [25] A. Niezgodá, D. Kajtoch, and E. Witkowska, Efficient two-mode interferometers with spinor Bose-Einstein condensates, *Phys. Rev. A* **98**, 013610 (2018).
- [26] S. Yi and L. You, Trapped condensates of atoms with dipole interactions, *Phys. Rev. A* **63**, 053607 (2001).
- [27] S. Yi, L. You, and H. Pu, Quantum Phases of Dipolar Spinor Condensates, *Phys. Rev. Lett.* **93**, 040403 (2004).
- [28] S. Yi and H. Pu, Magnetization, squeezing, and entanglement in dipolar spin-1 condensates, *Phys. Rev. A* **73**, 023602 (2006).
- [29] H. Xing, A. Wang, Q. S. Tan, W. Zhang, and S. Yi, Heisenberg-scaled magnetometer with dipolar spin-1 condensates, *Phys. Rev. A* **93**, 043615 (2016).
- [30] S. Giovanazzi, A. Görlitz, and T. Pfau, Tuning the Dipolar Interaction in Quantum Gases, *Phys. Rev. Lett.* **89**, 130401 (2002).
- [31] A. Griesmaier, J. Stuhler, T. Koch, M. Fattori, T. Pfau, and S. Giovanazzi, Comparing Contact and Dipolar Interaction in a Bose-Einstein Condensate, *Phys. Rev. Lett.* **97**, 250402 (2006).
- [32] J. Stuhler, A. Griesmaier, T. Koch, M. Fattori, T. Pfau, S. Giovanazzi, P. Pedri, and L. Santos, Observation of Dipole-Dipole Interaction in a Degenerate Quantum Gas, *Phys. Rev. Lett.* **95**, 150406 (2005).
- [33] H. Pu, W. Zhang, and P. Meystre, Ferromagnetism in a Lattice of Bose-Einstein Condensates, *Phys. Rev. Lett.* **87**, 140405 (2001).
- [34] W. Zhang, S. Yi, M. S. Chapman, and J. Q. You, Coherent zero-field magnetization resonance in a dipolar spin-1 Bose-Einstein condensate, *Phys. Rev. A* **92**, 023615 (2015).
- [35] Y. Huang, Y. Zhang, R. Lü, X. Wang, and S. Yi, Macroscopic quantum coherence in spinor condensates confined in an anisotropic potential, *Phys. Rev. A* **86**, 043625 (2012).
- [36] C. Chin, R. Grimm, P. Julienne, and E. Tiesinga, Feshbach resonances in ultracold gases, *Rev. Mod. Phys.* **82**, 1225 (2010).
- [37] C. W. Helstrom, *Quantum Detection and Estimation Theory* (Academic, New York, 1976).
- [38] A. S. Holevo, *Probabilistic and Statistical Aspects of Quantum Theory* (North-Holland, Amsterdam, 1982).
- [39] H. Strobel, W. Muessel, D. Linnemann, T. Zibold, D. B. Hume, L. Pezzè, A. Smerzi, and M. K. Oberthaler, Fisher information and entanglement of non-Gaussian spin states, *Science* **345**, 424 (2014).
- [40] J. Ma, Y. Huang, X. Wang, and C. P. Sun, Quantum Fisher information of the Greenberger-Horne-Zeilinger state in decoherence channels, *Phys. Rev. A* **84**, 022302 (2011).
- [41] J. Liu, H. Yuan, X. M. Lu, and X. Wang, Quantum Fisher information matrix and multiparameter estimation, *J. Phys. A: Math. Theor.* **53**, 023001 (2020).
- [42] G. Ferrini, D. Spehner, A. Minguzzi, and F. W. J. Hekking, Effect of phase noise on quantum correlations in Bose-Josephson junctions, *Phys. Rev. A* **84**, 043628 (2011).
- [43] Y. Huang, W. Zhong, Z. Sun, and X. Wang, Fisher-information manifestation of dynamical stability and transition to self-trapping for Bose-Einstein condensates, *Phys. Rev. A* **86**, 012320 (2012).
- [44] M. J. Holland and K. Burnett, Interferometric Detection of Optical Phase Shifts at the Heisenberg Limit, *Phys. Rev. Lett.* **71**, 1355 (1993).
- [45] P. Hyllus, O. Gühne, and A. Smerzi, Not all pure entangled states are useful for sub-shot-noise interferometry, *Phys. Rev. A* **82**, 012337 (2010).
- [46] B. Lücke, Twin matter waves for interferometry beyond the classical limit, *Science* **334**, 773 (2011).
- [47] W. Wiczcerek, R. Krischek, N. Kiesel, P. Michelberger, G. Tóth, and H. Weinfurter, Experimental Entanglement of a Six-Photon Symmetric Dicke State, *Phys. Rev. Lett.* **103**, 020504 (2009).
- [48] G. Tóth, Entanglement detection in optical lattices of bosonic atoms with collective measurements, *Phys. Rev. A* **69**, 052327 (2004).